Journal of Cell Science 113, 3573-3582 (2000)
Printed in Great Britain © The Company of Biologists Limited 2000
JCS1781

Use of phosphosynapsin I-specific antibodies for image analysis of signal transduction in single nerve terminals

Andrea Menegon[1,*], David D. Dunlap[1,*], Francesca Castano[1], Fabio Benfenati[2], Andrew J. Czernik[3], Paul Greengard[3] and Flavia Valtorta[1,‡]

[1]Dept Neuroscience, San Raffaele Scientific Institute, Milan, Italy
[2]Dept Experimental Medicine, Section of Physiology, University of Genoa, Genoa and Dept Neuroscience, University of Rome Tor Vergata, Rome, Italy
[3]Laboratory of Molecular and Cellular Neuroscience, The Rockefeller University, New York, USA
*These two authors contributed equally to the work
‡Author for correspondence (e-mail: valtorta.flavia@hsr.it)

Accepted 22 August; published on WWW 4 October 2000

SUMMARY

We have developed a semi-quantitative method for indirectly revealing variations in the concentration of second messengers (Ca^{2+}, cyclic AMP) in single presynaptic boutons by detecting the phosphorylation of the synapsins, excellent nerve terminal substrates for cyclic AMP- and Ca^{2+}/calmodulin-dependent protein kinases. For this purpose, we employed polyclonal, antipeptide antibodies recognising exclusively synapsin I phosphorylated by Ca^{2+}/calmodulin-dependent protein kinase II (at site 3) or synapsins I/II phosphorylated by either cAMP-dependent protein kinase or Ca^{2+}/calmodulin-dependent protein kinase I (at site 1). Cerebellar granular neurones in culture were double-labelled with a monoclonal antibody to synapsins I/II and either of the polyclonal antibodies. Digitised images were analysed to determine the relative phosphorylation stoichiometry at each individual nerve terminal. We have found that: (i) under basal conditions, phosphorylation of site 3 was undetectable, whereas site 1 exhibited some degree of constitutive phosphorylation; (ii) depolarisation in the presence of extracellular Ca^{2+} was followed by a selective and widespread increase in site 3 phosphorylation, although the relative phosphorylation stoichiometry varied among individual terminals; and (iii) phosphorylation of site 1 was increased by stimulation of cyclic AMP-dependent protein kinase but not by depolarisation and often occurred in specific nerve terminal sub-populations aligned along axon branches. In addition to shedding light on the regulation of synapsin phosphorylation in living nerve terminals, this approach permits the spatially-resolved analysis of the activation of signal transduction pathways in the presynaptic compartment, which is usually too small to be studied with other currently available techniques.

Key words: Synapsin, Phosphorylation, Cyclic AMP, Ca^{2+}, Synaptic vesicle

INTRODUCTION

The presynaptic nerve terminal is a key compartment for communication within the nervous system. In fact, interneuronal communication is achieved primarily via the exocytotic release of neurotransmitters from synaptic vesicles present in nerve terminals. Physiologically, neurotransmitter release is elicited by the arrival of an action potential at a nerve terminal. This results in membrane depolarisation and a subsequent rise in the sub-plasmalemmal concentration of Ca^{2+}, which is sufficient to stimulate release (Katz and Miledi, 1965; Ceccarelli and Hurlbut, 1980; Valtorta and Benfenati, 1995).

It has long been known that the process of neurotransmitter release is a highly plastic phenomenon, which is sensitive to the previous history of the synapse, and can be adjusted in an extremely prompt way to changes in the intra- and extracellular environment (Jessell and Kandel, 1993). Although this feature is of paramount importance for information processing in the central nervous system and for adjusting the level of efficiency of a synapse to the physiological needs of a neurone, the bases for the high modulability of release are not completely understood. Variations in the amount of the neurotransmitter released reflect variations in the number of synaptic vesicles which undergo exocytosis following an action potential, and are caused by changes in either the number of synaptic vesicles which are immediately available for fusion or the probability of each vesicle to fuse with the plasma membrane following Ca^{2+} entry (Boyd and Martin, 1956). Modulation of neurotransmitter release is thought to be achieved through fluctuations in the intra-terminal levels of second messengers such as Ca^{2+} or cAMP, which in turn activate the phosphorylation of specific protein substrates by protein kinases (Llinas et al., 1981; Smith and Augustine, 1988; Zucker, 1989; Weiner, 1979). Thus far the study of signal transduction in nerve terminals has been hampered by the tiny

dimensions of this compartment. Indeed, the dimensions of most synaptic terminals (0.5-5 μm in width) are such that they are very difficult to access by direct biophysical and biochemical analysis. Also the optical evaluation of second messenger levels (e.g. Ca^{2+}) by fluorescent probes (Grynkiewicz et al., 1985) does not yield conclusive results, since the resolution of the technique does not allow discrimination of the pre-and post-synaptic contributions to the signal. On the other hand, the biochemical analysis of subcellular fractions such as synaptosomes has the disadvantage that it lacks spatial resolution and that these fractions are not entirely presynaptic (Dunkley et al., 1988).

One possible strategy to overcome these problems is that of indirectly evaluating changes in the presynaptic levels of second messengers by measuring the phosphorylation of proteins specific to this compartment and subjected to phosphorylation by second messenger-activated protein kinases. Among the nerve terminal-specific phosphoproteins, the synapsins are ideal candidates, since they are exclusively confined to the presynaptic compartment and are at the convergence of multiple signalling pathways (for recent reviews, see Valtorta et al., 1998; Hilfiker et al., 1999).

The synapsins are abundant synaptic vesicle-associated phosphoproteins that are thought to tether synaptic vesicles to each other as well as to the actin cytoskeleton, thus maintaining a reserve pool of vesicles in the proximity of the release sites (De Camilli et al., 1990; Valtorta et al., 1992a; Greengard et al., 1993). In vertebrates, the synapsins are encoded by three distinct genes (synapsins I, II and III), each of which undergoes alternative splicing to generate distinct isoforms (Südhof et al., 1989; Kao et al., 1998; Hosaka and Südhof, 1998). The major structural differences among the various synapsin isoforms are restricted to the COOH-terminal region of the molecules, whereas the NH_2-terminal regions are largely conserved (Hilfiker et al., 1999). At the NH_2 terminus, a consensus phosphorylation site for cAMP-dependent protein kinase (PKA) and Ca^{2+}/calmodulin-dependent protein kinase (CaMPK) I (site 1) is present in all isoforms (Huttner and Greengard, 1979; Czernik et al., 1987; Kao et al., 1998). In synapsins I and II, this site has been shown to undergo phosphorylation in response to increased levels of second messengers (Huttner and Greengard, 1979; Huttner et al., 1981). Synapsin I, but not synapsin II, also exhibits two sites of phosphorylation for CaMPKII (sites 2,3; Huttner and Greengard, 1979; Czernik et al., 1987). Interestingly, phosphorylation of synapsin I at these sites causes a marked conformational change in the molecule (Benfenati et al., 1990) that decreases its ability to interact with both actin and the synaptic vesicle membrane (Schiebler et al., 1986; Bähler and Greengard, 1987; Petrucci and Morrow, 1987; Benfenati et al., 1989; Valtorta et al., 1992b). In addition, synapsin I has been shown to undergo phosphorylation by mitogen-activated protein kinase Erk 1/2 at three sites (sites 4, 5 and 6). Site 6 is also phosphorylated by cyclin-dependent kinase 5 (Jovanovic et al., 1996; Matsubara et al., 1996). Because the synapsins become phosphorylated at distinct sites in response to variations in different second messengers, it should be possible to use antibodies which specifically recognise the various phosphorylated forms of the synapsins as detectors for the activation of specific kinases, and hence of specific signal transduction pathways.

We have developed a microscopic method in which various phosphorylated forms of the synapsins are immunocitochemically double-labelled with phosphorylation state-specific and phosphorylation state-insensitive antibodies to determine changes in their apparent phosphorylation stoichiometry as an indication of the variations in second messenger levels in individual nerve terminals. We have found that phosphorylation of the synapsins at sites 1 and 3 under basal conditions and in response to stimuli that increase the intra-terminal levels of Ca^{2+} or cAMP varies considerably in terms of both extent of phosphorylation and number and spatial distribution of the nerve terminals involved.

MATERIALS AND METHODS

Materials

Reagents were from the following sources: peroxidase-conjugated antibodies and chemiluminescence detection system, Amersham Life Sciences Inc. (Buckinghamshire, England); polyacrylamide, Bio-Rad Laboratories (Hercules, California); Hanks' balanced salt solution without Ca^{2+} or Mg^{2+}, glutamate, Dulbecco's modified Eagle medium (DMEM) without glutamate, Boehringer Ingelheim Biowhittaker (Verviers, Belgium); Tris-HCl, Boehringer Mannheim (Germany); Sprague Dawley rats, Charles River (Calco, Italy); 4-aminopyridine (4AP), bovine pancreas deoxyribonuclease I, W7, Calbiochem (La Jolla, California); paraformaldehyde, Electron Microscopy Sciences (Fort Washington, Pennsylvania); fetal calf serum, HyClone (Aalst, Belgium); fluorescein-conjugated goat anti-mouse and tetramethyl rhodamine-conjugated donkey anti-rabbit antibodies, Jackson Immunoresearch Laboratories (West Grove, Pennsylvania); penicillin-streptomycin, goat serum, Life Technologies, Inc. (Rockville, Maryland); BCA protein assay reagent, Pierce Chemical Co. (Rockford, Illinois); KN62, Research Biochemicals International (Natick, Maryland); cytosine-1-β-D-arabinofuranoside, forskolin, dibutyryl cAMP, and monoclonal anti-glial fibrillary acidic protein (GFAP), Sigma Chemical Co. (St Louis, Missouri). All other chemicals were of reagent grade from standard commercial suppliers. The anti-synapsin monoclonal antibody, 19.11, and the phosphorylation state-specific anti-synapsin polyclonal antibodies, RU19 and G257, were obtained and affinity-purified as described (Czernik et al., 1991; Vaccaro et al., 1997). Synapsin I was purified from bovine brain as described by Schiebler et al. (1986), and modified by Bähler and Greengard (1987). Purified dephosphorylated synapsin I was phosphorylated either by the catalytic subunit of PKA (site 1) or by CaMPKII (sites 2 and 3) as described by Schiebler et al. (1986).

Tissue dissociation and cell culture

Cerebellar granule cells were prepared according to the method of Gallo et al. (1987), modified as previously described (Menegon et al., 1997). In brief, cerebella of 5-day-old Sprague Dawley rats were dissected in Ca^{2+} and Mg^{2+}-free Hanks' solution on ice, manually sliced (6-7 slices per cerebellum), then transferred into the same medium supplemented with trypsin (1 mg/ml) and DNAse I (0.5 mg/ml), and incubated for 10 minutes at 37°C. At the end of the enzyme treatment, slices were washed twice with Hanks' solution, and then trypsin activity was blocked by incubation for 10 minutes at 37°C in DMEM supplemented with 10% foetal calf serum. After two washes in Hanks' solution, the cells were triturated in a 10-ml pipette. The cell suspension was then centrifuged at 120 ***g*** for 10 minutes and the pellet was resuspended in DMEM supplemented with 10% foetal calf serum, 2 mM glutamine, 100 UI/ml penicillin, and 100 μg/ml streptomycin. Finally, the cells were plated on previously prepared poly-L-ornithine-coated glass coverslips. In order to favour neuronal

survival and growth, 3 days after plating cells were transferred into the same medium supplemented with 10 mM KCl which also contained 10 μM cytosine-1-β-D-arabinofuranoside to prevent glial cell proliferation. The medium was replaced every 5 days.

Stimulation of cells

All the experiments were performed at 37°C as follows. Cells were incubated in either experimental or control conditions for a total of 30 minutes beginning with the exchange of the culture medium for Krebs Ringer's-HEPES (KRH) buffer (130 mM NaCl, 5 mM KCl, 1.2 mM $MgSO_4$, 1.2 mM KH_2PO_4, 2 mM $CaCl_2$, 1.1 mg/ml glucose and 25 mM HEPES, pH 7.4). At the indicated time points, KRH was completely replaced with the same medium containing stimulatory and/or inhibitory agents. At the end of the stimulation period, the cells were rapidly washed in KRH supplemented with 2 mM EGTA and either lysed for immunoblotting or chemically fixed for immunofluorescence experiments. The concentrations of stimulating agents and the times of exposure of the cells to them were optimised to maximise the resulting phosphorylation.

Immunoblot analysis

After the experimental treatments, the cells were lysed and scraped from the coverslips in a buffer containing 1% sodium dodecyl sulfate (SDS), 2 mM EDTA, 10 mM HEPES (pH 7.4), and immediately frozen in liquid nitrogen. After thawing, lysates were boiled and sonicated. Equal amounts of protein were electrophoresed through SDS-8.5% polyacrylamide gels after dilution in Laemmli's 'stop buffer' (Laemmli, 1970) and transferred to nitrocellulose as previously described (Burgaya et al., 1995). The filters were then blocked for 2 hours in blocking solution (TBS: 5% non-fat dry milk in 200 mM NaCl, 50 mM Tris-HCl, pH 7.4) at room temperature, washed twice in TBS, and incubated overnight at 4°C with the primary antibodies in blocking solution supplemented with 0.1% Triton X-100. After three washes in TBS with 0.1% Triton X-100, the filters were incubated with the secondary antibody for two hours at room temperature, washed 5 times in TBS with 0.1% Triton X-100 for 5 minutes each and finally developed using enhanced chemiluminescence detection.

Immunofluorescence experiments

Cells were fixed for 30 minutes at 37°C in 4% formaldehyde (freshly prepared from paraformaldehyde) dissolved in 120 mM sodium phosphate buffer, pH 7.4, with 4% sucrose and 4 mM EGTA. After fixation, cells were washed twice in 180 mM NaCl, 10 mM sodium phosphate buffer, pH 7.4 (PBS), then once in 500 mM NaCl, 20 mM sodium phosphate buffer (high salt solution) and incubated with the antibodies in a solution containing: 15% goat serum, 0.3% Triton X-100, 20 mM sodium phosphate buffer, pH 7.4, and 450 mM NaCl. Between successive incubations with antibodies, the cells were washed three times for 10 minutes each in high salt solution. After the final incubation, the cells were washed twice in high salt solution for 10 minutes each, once in PBS and finally once in 5 mM sodium phosphate buffer, pH 7.4. Cells were mounted in 70% glycerol, 180 mM NaCl and 10 mM sodium phosphate buffer, pH 7.4, containing 1 mg/ml of phenylenediamine to minimise bleaching.

Image acquisition

Multi-color fluorescence and differential interference contrast images were acquired for overlay using a Zeiss Axiovert 135 microscope equipped with a digital video camera (model C4247-98, Hamamatsu Photonics, Hamamatsu City, Japan).

For digital analysis of immunofluorescence, specimens were viewed through a Planapo ×63/1.4 oil immersion objective with illumination from a 50 watt mercury vapour arc lamp through an infrared-blocking glass filter. The microscope was equipped with fluorescein (exciter 450-490, dichroic 505, emitter 525-575) and rhodamine (exciter 546/12, dichroic 565, emitter 580 LP) fluorescence filters and a Hamamatsu (Hamamatsu City, Japan) C2400-8 SIT video camera connected either to a Macintosh IIci personal computer via a DT-2255-50Hz frame grabber from Data Translation (Marlboro, Massachusetts) or to an AST P/75 personal computer via an LG3 frame grabber from Scion Corporation (Frederick, Maryland).

For a single field of view, fluorescence images of both fluorochromes were digitised using the SIT camera. The gain, offset, and sensitivity settings of the camera controller were maintained constant for recording from each single field of view with the two different filter cubes, but were adjusted to optimise the signal intensity range for different fields of view. If the intensities of the phospho-synapsin and total synapsin signals differed significantly for stimulated synapses, neutral density filters were inserted into the illumination light path when recording images of the stronger signal, to permit optimisation of the dynamic range of the camera for both signals. This procedure was then adopted for all coverglasses prepared in that experiment. Using the public-domain image analysis program NIH Image (developed at the U.S. National Institutes of Health, Bethesda, Maryland, and available at http://rsb.nih.gov/nih-image), the pairs of images were analysed to establish fluorescence intensity ratios between phosphorylated and total synapsin, indicative of the extent of synapsin I (or I and II) phosphorylation under various incubation conditions. The digitised intensity levels ranged over 40-255 for the DT-2255-50Hz framegrabber and 0-255 for the LG3 framegrabber.

Immunofluorescence ratio analysis

Image processing was accomplished with user-written routines for NIH Image. For each pair of images, an alignment was performed based on a fast Fourier transform-based cross correlation. The position of the peak of the cross correlation was determined and the synapsin image was shifted into alignment with the phospho-synapsin image. Subsequently, histograms of pixel intensities were calculated for each image in a pair. As expected for dark images with many small bright spots, each histogram exhibited a large peak at the background level in the image. The mode value of this peak less the standard deviation of the synapsin mode peak was subtracted from each pixel in the two images to establish a common background level between the phospho-synapsin and synapsin images. Then the ratio, a real number, of the phospho-synapsin to synapsin intensity was calculated for each point in the field of view. This ratio image was averaged by replacing each pixel with the mean of itself and the eight neighbouring pixels.

Spots to be interpreted as synapses were then defined using the image of the total synapsin label. Once again the histogram of the anti-synapsin image was calculated to identify the background level. The sum of the mode and the standard deviation of the distribution about the mode value was subtracted from every point in the image. Then a convolution with a two-dimensional, 5×5 Laplace filter was performed to fracture large spots into their component synapses. The resulting image was then used to create a binary image with a large background (level 0) dotted with the locations of pixels corresponding to small synapses (non-zero levels). Spots of a lateral size above or below user specified minima or maxima (4 and 25) were then erased from the mask as were any spots for which the corresponding total synapsin or phospho-synapsin fluorescence signals were saturated. This binary mask was used to select synapses to be analysed in the ratio image.

For each condition in an experiment, a data set was constructed of pixels corresponding to the maximum ratio within identified synapses. In the analysis of each experiment, the control or basal condition was examined first. The mean phosphorylated/total synapsin ratio for synapses under basal conditions was subsequently used to normalise all data in the experiment. Thus, the ratio for each synapse in the analysis was divided by the mean ratio for synapses in images recorded for neurones under basal conditions to derive a unitless 'multiple of basal phosphorylation' (MBP). To effectively summarise the results, such MBPs for synapses in any particular condition were

analysed in percentage and cumulative percentage histograms as shown in Fig. 5. Although MBP values calculated by computer analysis cannot be interpreted as actual stoichiometries of phosphorylation, since they do not take into account the efficiency of primary and secondary antibody labelling, they provide a reliable semi-quantitative indication of the mean phosphorylation level of synapsin in a given bouton.

The interactive/automated analysis routines also output a non-normalised ratio data image for each field of view to permit a spatial analysis of synapsin phosphorylation in individual synapses. This image was normalised following the analysis to generate colour-coded, spatially resolved information as shown in Figs 4 and 7.

RESULTS

Immunoblot detection of synapsin I phosphorylation on phosphorylation site 3

In order to investigate the signal transduction pathways operating within nerve terminals of cerebellar granule cells in culture, polyclonal antibodies that recognise the synapsins phosphorylated on specific residues were used in combination with a monoclonal anti-synapsin antibody. The specificity of the polyclonal antibodies was demonstrated by comparing immunoblots containing increasing amounts of either dephosphorylated, PKA-phosphorylated, or CaMPKII-phosphorylated purified bovine synapsin I. The monoclonal antibody 19.11, whose epitopes are distinct from the sequences encompassing phosphorylation sites 1,2 and 3 (Vaccaro et al., 1997), recognises synapsins I and II independently of their state of phosphorylation. In contrast, the polyclonal antibodies RU19 (directed against a phospho-peptide containing phosphorylated site 3) and G257 (directed against a phospho-peptide containing phosphorylated site 1) specifically recognise synapsin I phosphorylated by CaMPKII and synapsins I/II phosphorylated by PKA, respectively (Fig. 1A).

Immunoblots of cerebellar granule cells solubilised either under resting conditions or after K^+-induced depolarisation in the absence or presence of extracellular Ca^{+2} were probed with the anti-synapsin and the anti-phosphorylation-site 3 antibodies. As shown in Fig. 1B, only lysates of granule cells depolarised in the presence of extracellular Ca^{2+} contained significant amounts of phosphorylated synapsin I. Similar results were obtained when cultured granule cells were depolarised with 4AP. Maintenance of the state of synapsin phosphorylation during lysis was achieved only if extracellular Ca^{2+} was removed prior to solubilisation by quickly rinsing the cells with buffer containing 2-4 mM EGTA. In fact, during lysis, vast amounts of Ca^{+2} may enter the cells very quickly and undermine the stabilising action of the lysis buffer through rapid activation of protein kinases and phosphatases.

Immunofluorescence detection of synapsin I phosphorylation on phosphorylation site 3

In order to characterize the organization of the neurons in our cultures, cells were visualized with Nomarski optics and doubly stained with anti-GFAP and anti-synapsin antibodies. Fig. 2 shows that synaptic boutons, as outlined by anti-synapsin staining, were lying along neurites, and did not show any preferential association with glial cells.

For the spatial analysis of synapsin I phosphorylation on site 3, granule cells were treated as described above, fixed and stained by double indirect immunofluorescence with anti-synapsin and anti-phosphorylation-site 3 antibodies. The resulting immunofluorescence micrographs for the anti-synapsin antibody clearly revealed a typical synaptic pattern of staining in both resting and stimulated samples (Fig. 3). In contrast, after stronger stimulation (70 mM KCl) the synapsins appeared to diffuse away from synapses (data not shown). The staining that resulted from labelling with the anti-phosphorylation-site 3 antibody was significantly above background only in cells exposed to KCl or 4AP in the presence of extracellular Ca^{+2}. Depolarisation of granule cells with 3 mM 4AP in the presence of extracellular Ca^{+2} for 1 minute provoked extensive phosphorylation of synapsin I at site 3. Under these conditions, a typical synaptic pattern was found comparable to that observed with the anti-synapsin antibody. As in the case of immunoblots, for immunofluorescence it was critical to remove extracellular Ca^{+2} prior to fixation to avoid a rapid influx of the ion that would have blurred the differences in phosphorylation. In order to assess whether the increased labelling observed with anti-phosphorylation-site 3 antibodies after 4AP stimulation was indeed attributable to CaMPKII-mediated synapsin I phosphorylation, in some experiments cells were treated with

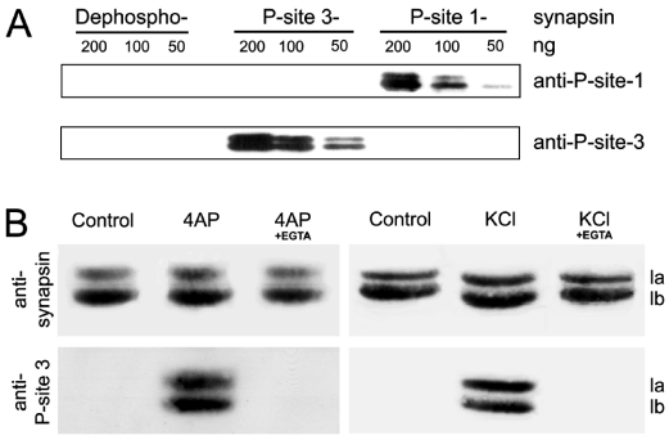

Fig. 1. (A) Specificity of the phospho-specific antibodies. 200, 100, and 50 nanograms of purified bovine synapsin I either dephosphorylated, phosphorylated on site 1 by the catalytic subunit of PKA, or phosphorylated on sites 2 and 3 by CaMPKII were electrophoresed through an SDS-8.5% polyacrylamide gel. After transfer to nitrocellulose, the protein blot was labelled with either anti-phosphorylation site 1 (anti-P-site1) or anti-phosphorylation site 3 (anti-P-site3) antibodies, followed by horseradish peroxidase-conjugated secondary antibodies and chemiluminescence detection. (B) Immunoblot analysis of 4AP- and KCl-induced phosphorylation of synapsin I at site 3. Cerebellar granule cells (12 days in culture) were incubated for 30 minutes in KRH. During the final 1 or 2 minutes of incubation, the solution was replaced with KRH containing either 3 mM 4AP or 55 mM KCl in the absence or presence of either 2 mM $CaCl_2$ or 2 mM $MgCl_2$/2 mM EGTA. Control: sample incubated with KRH without stimulatory agents. After lysis, proteins (100 μg/lane) were electrophoresed through an SDS-8.5% polyacrylamide gel, transferred to nitrocellulose, and labelled with either anti-synapsin (upper panel) or anti-phosphorylation site 3 (lower panel) antibodies followed by horseradish peroxidase-conjugated secondary antibodies and chemiluminescence detection.

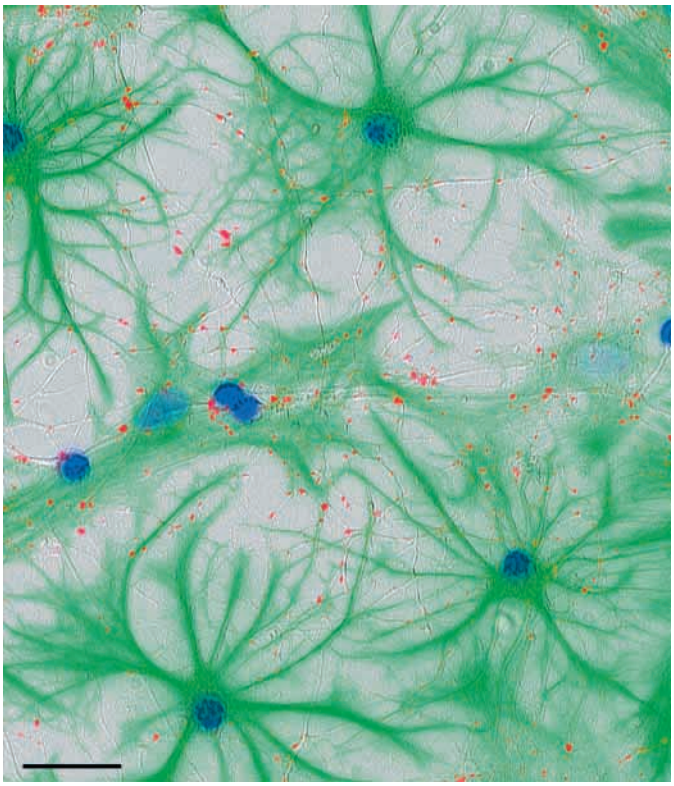

Fig. 2. Differential interference contrast image of cerebellar granule cells (12 days in culture). Superimposed on the image are the fluorescence images of synapsin (red) and GFAP (green) antibody stainings. Synaptic boutons form along neurites with or without underlying astrocytes. Nuclei are outlined by staining with the Hoechst 33258 dye (blue). Bar, 10 μm.

either W7, a potent inhibitor of calmodulin (Itoh and Hidaka, 1984) or KN62, which, at the concentration used, is a specific inhibitor of CaMPKII (Schweitzer et al., 1995). Pre-stimulus incubation with either inhibitor greatly reduced the immunocitochemically-detected phosphorylation of site 3 on synapsin I. Similar results were obtained in the case of stimulation with high K^+ (data not shown).

Quantitation of the relative phosphorylation of synapsin I in individual synapses

In order to obtain a semi-quantitative estimate of the phosphorylation of synapsin I on site 3, immunofluorescence images were recorded with a video camera, digitised with a frame grabber, and analysed. The procedure for analysis identified synapses in the anti-synapsin image as spots within a fixed size range with fluorescence intensity above a certain threshold. Ratios of the anti-phosphorylation site 3 intensity to the anti-synapsin intensity were then computed for each pixel in the spots corresponding to synapses. The maximum value for each spot in a smoothed image of these ratios was taken as the relative phosphorylation of synapsin I in the synapse corresponding to that spot. These relative values were satisfactory for comparisons among differently treated specimens derived from cells from the same dissection, culture, experiment and immunofluorescence labelling. A further normalisation was necessary to compare the levels of synapsin I phosphorylation in specimens from separate experiments, because the relative intensities of immunofluorescence staining for the two antigens varied slightly. A normalisation was performed using the average, relative phosphorylation of synapsin I for synapses in all fields of view recorded from non-depolarised specimens. Following normalisation, each pixel was assigned a value corresponding to multiples of the basal synapsin I phosphorylation and a pseudo-colour image was produced revealing the pixel-by-pixel variation within and between synapses.

As shown in Fig. 4, depolarisation with 55 mM KCl for two minutes significantly increased synapsin I phosphorylation in most synapses, with multiples of basal phosphorylation for individual synapses ranging from 1 to 4. Chelation of extracellular Ca^{2+} blocked the increase in phosphorylation and under this condition the range of multiples of basal phosphorylation was similar to that of the control condition.

Distribution of the relative phosphorylation of synapsin I in populations of synapses

The frequency distribution of MBP values grouped in selected ranges was analysed in control and KCl-stimulated specimens (Fig. 5, left panels). For the control conditions, the distribution of MBP values displayed one almost symmetrical peak with a small percentage of synapses that had more highly phosphorylated synapsin I. A similar distribution was observed for samples depolarised in the presence of EGTA. In both cases the distributions reached a peak slightly below one, due to the influence of a small number of synapses with highly phosphorylated synapsin I on the mean value used in the normalisation. From the analysis of the cumulative distributions, it appeared that only 10% of synapses under control conditions had MBP ratios above 1.75 (90th percentile=1.75 MBP). Potassium-induced membrane depolarisation caused a significant shift of the cumulative curve to the right (90th percentile=3.8 MBP). Using the value of the 90th percentile under basal conditions as a threshold above which a synapse is considered to contain synapsin I phosphorylated above control, KCl-induced membrane depolarisation caused significant synapsin I phosphorylation in an additional 40% of the total number of synapses.

The middle panels in Fig. 5 depict a similar set of histograms calculated from a representative experiment of several experiments in which 4AP was used to depolarise the cell membrane. The distributions for both the control condition and for the depolarisation in the absence of external Ca^{2+} were similar to those observed with KCl-induced depolarisation (90th percentile=1.25 MBP). Membrane depolarisation by 4AP caused significant right-shift of the cumulative curve that was more pronounced than the effect observed with KCl (90th percentile=4.8 MBP). Using the value of the 90th percentile under basal conditions as a threshold (see above), 4AP caused a significant synapsin I phosphorylation in an additional 78% of synapses. Furthermore, the distribution appeared broader than that resulting from KCl-induced depolarisation, revealing the presence of a larger percentage of synapses containing highly phosphorylated synapsin I.

cAMP or forskolin-induced phosphorylation of synapsins on phosphorylation site 1

After depolarisation of granule cells by either high extracellular K^+ or 4AP, no significant changes in synapsin site

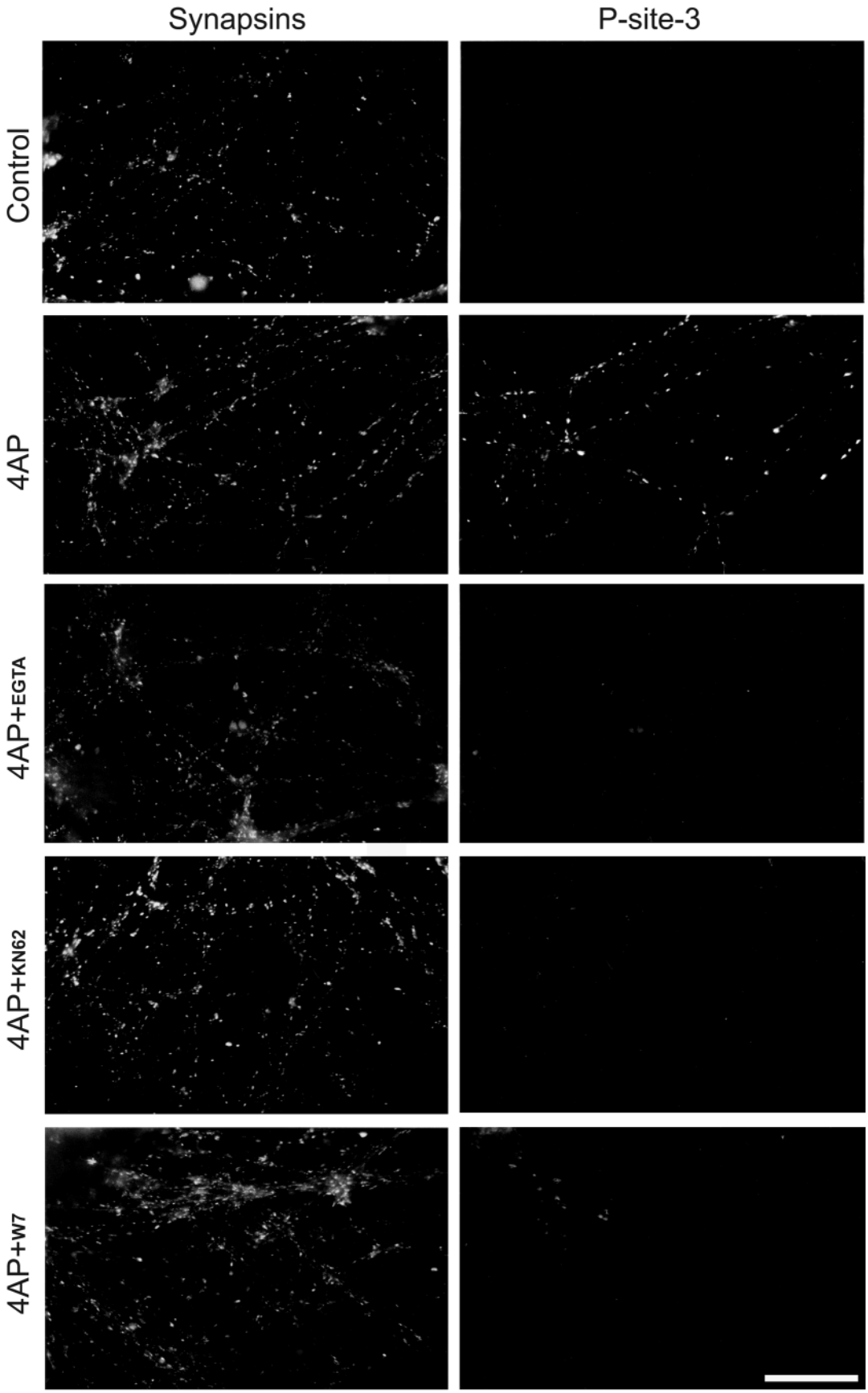

Fig. 3. Immunofluorescence detection of 4AP-induced phosphorylation of synapsin I at P-site 3. Cerebellar granule cells (12 days in culture) were incubated for 30 minutes in KRH. During the final 1 minute of incubation, the solution was replaced with KRH containing 3 mM 4AP in the absence or presence of either 2 mM $CaCl_2$ or 2 mM $MgCl_2$/2 mM EGTA. Control: sample incubated with KRH without stimulatory agents. In some samples, after a 15-minute incubation with KRH the medium was replaced with KRH containing either 2 μM KN62 or 50 μM W7, and finally with KRH containing 3 mM 4AP in the absence or presence of the same inhibitor (4AP+KN62, or 4AP+W7). After formaldehyde fixation, double immunofluorescence was used to reveal total synapsins and P-site 3-phosphorylated synapsin I. Bar, 34 μm.

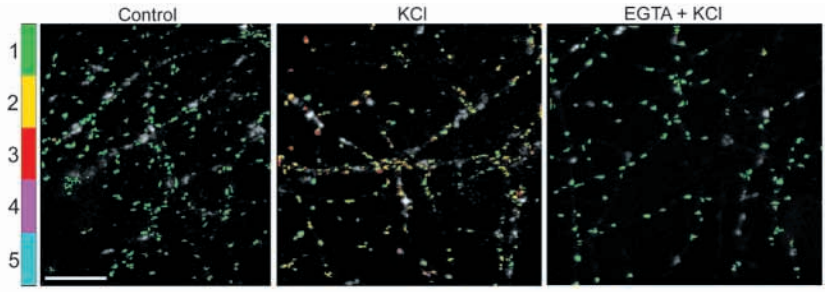

Fig. 4. Immunofluorescence-ratio imaging of KCl-induced phosphorylation of synapsin I at site 3. Cerebellar granule cells were stimulated and processed for immunofluorescence as described in the legend to Fig. 1B. The extent of site 3 phosphorylation in individual synapses was quantified in digitised immunofluorescence images. Colour-coding of the synapses indicates the MBP, i.e. the average ratio of phosphorylation site 3 and synapsin immunofluorescence normalised against control conditions. White-coloured spots were excluded from the analysis. Bar, 25 μm.

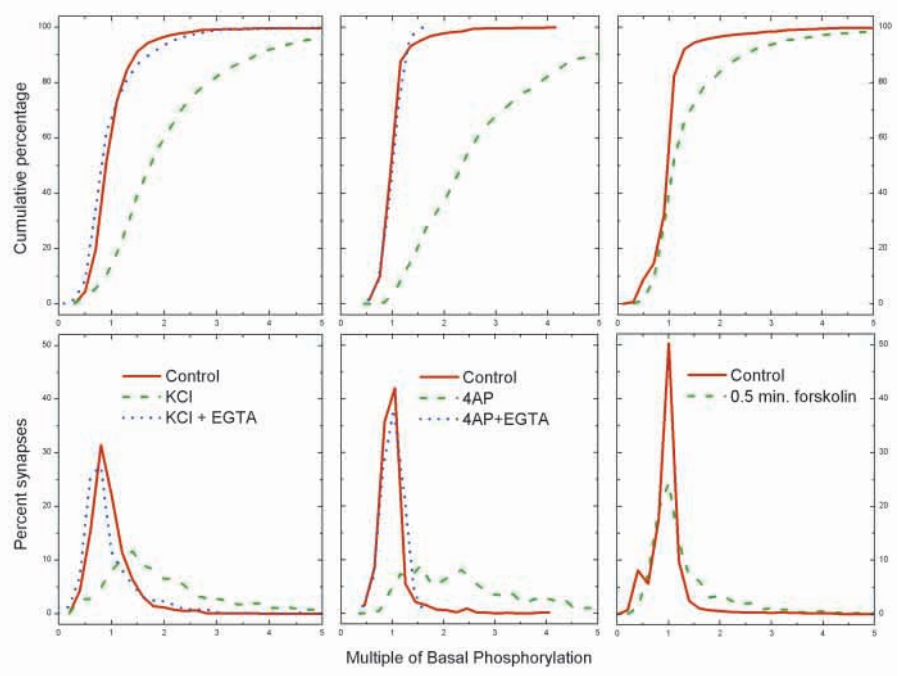

Fig. 5. Quantitative analysis of KCl, 4AP and forskolin-induced phosphorylation of the synapsins. Left and middle panels: cells were treated as described in the legend to Fig. 1B. Right panels: during the final 0.5 minutes of incubation the samples were treated with KRH containing 10 μM forskolin. Populations of synapses with various levels of synapsin phosphorylation were characterised by automated analysis of digitised images. The lower graphs are frequency distributions of the multiple of the basal phosphorylation values for individual synapses. These data are represented cumulatively in the upper graphs. Left panel: 4 separate experiments with 4 to 6 fields of view for each condition containing 87 to 134 synapses/field; Middle panel: 1 experiment with 4 (KRH and 4AP) or 8 (EGTA + 4AP) fields of view containing 222 to 108 synapses/field; Right panel: 2 experiments with 5 to 8 fields of view for each condition containing 232 (KRH) or 164 (forskolin) synapses/field.

1 phosphorylation were detected by either immunoblotting or immunofluorescence (data not shown). In contrast, an increase in the site 1 phosphorylation of synapsins I and II was observed after treatment with either 10 μM forskolin or 10 mM dibutyryl cAMP (Fig. 6). Taken together, these results suggest that in our preparation, although phosphorylation of site 1 by CaMPKI was apparently not affected by depolarisation, stimulation of PKA promoted a significant phosphorylation of the synapsins on this site. It is also interesting to note that a substantial level of synapsin site 1 phosphorylation was present under control conditions.

Distribution of the relative phosphorylation of the synapsins on phosphorylation site 1

Immunofluorescence images of site 1 phosphorylation versus total synapsin staining were quantified as described above for site 3 phosphorylation (Fig. 5, right panels). Under control conditions, the distribution of the MBP values was centred on one, with a small group of synapses containing synapsin with less-than-average site 1 phosphorylation and only 10% of all synapses having MBP values above 1.25 (90th percentile=1.25 MBP). Activation of PKA with either forskolin or dibutyryl cAMP induced a slight rightward shift of the cumulative curve (90th percentile=2.45 MBP). Using the value of the 90th percentile under basal conditions as a threshold, PKA activation promoted site 1 phosphorylation in an additional 25% of synapses. To further characterise this limited response within the population of synapses, the images of the MBP values were examined with the aim of determining if the responding synapses were neighbours or were randomly dispersed. Indeed, higher phosphorylation-site 1 staining was common to synapses lying along selected neurites, while synapses arrayed along other neurites were unresponsive to PKA activation. The synapsin and site 1 phosphorylation images shown in Fig. 7 represent examples in which the synapses along certain neurites failed to phosphorylate site 1 in response to forskolin, while synapses on nearby neurites showed increased site 1 phosphorylation. Similarly grouped synapses were found for cells analysed following dibutyryl cAMP treatment (data not shown). The selective response was not due to the presence or absence of glial cells in the various regions of the Petri dish, since we were unable to show any correlation between labelling with G257 and staining with glia-specific markers (data not shown).

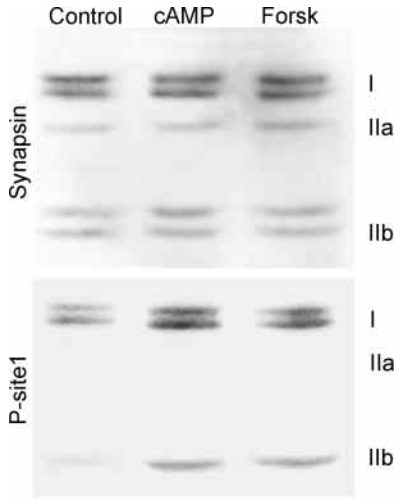

Fig. 6. Immunoblot analysis of dibutyryl-cAMP- or forskolin-induced phosphorylation of the synapsins at site 1. Cerebellar granule cells were incubated for 30 minutes in KRH (Control). In some samples (Forsk), during the final 0.5 minutes of incubation the medium was replaced with KRH containing 10 μM forskolin. In other samples (cAMP) during the final 10 minutes of incubation the medium was replaced with KRH containing 10 mM dibutyryl cAMP. After lysis, proteins (100 μg/lane) were electrophoresed through an SDS-8.5% polyacrylamide gel, transferred to nitrocellulose, and the blot was labelled with either anti-total synapsin (upper panel) or anti-phosphorylated-site 1 (lower panel) antibodies.

DISCUSSION

The synapsins were discovered as major phosphoproteins in the brain (for reviews, see De Camilli et al., 1990; Greengard et al., 1993; Valtorta et al., 1998; Hilfiker et al., 1999). In early investigations, phosphorylation of the synapsins was studied with conventional techniques, such as in vivo labelling (i.e. tracing the incorporation of ^{32}P from pre-labelled endogenous ATP into proteins) or 'back-phosphorylation' (i.e. studying the state of protein phosphorylation by measuring the amount of ^{32}P that can be incorporated into extracted proteins in the presence of exogenous kinases and radioactive ATP (Nestler and Greengard, 1984). More recently, antibodies which specifically recognise the various phosphorylated forms of the synapsins have been produced and proven useful for the analysis of synapsin I phosphorylation (Czernik et al., 1991; Jovanovic et al., 1996). When used in immunoblotting experiments, these antibodies provide information similar to that obtained with the other techniques, but their use is simpler. In addition, they offer the advantage of allowing the immediate identification not only of the increase in the phosphate content, but also of the precise site on which phosphorylation has occurred.

In immunoblots of cell lysates from cultures of cerebellar granular neurons, the RU19 antibody, specific for the phosphorylated serine 503 of rat synapsin I, selectively labelled the lanes containing the samples lysed after treatment with either KCl or 4AP in the presence of extracellular Ca^{2+}. These immunoblots confirmed previous findings indicating that in resting nerve terminals synapsin I is present in the dephosphorylated state and that the Ca^{2+} influx that accompanies membrane depolarisation activates CaMPKII to phosphorylate synapsin I on sites 2 and 3. The inherent disadvantage of immunoblotting of cellular lysates is that the cellular context of proteins is completely unknown. In addition, with this technique it is not possible to study the spatial distribution of phosphorylation in different cells or terminals in the preparation. In an attempt to assess the phosphorylation of synapsins in situ, the phospho-specific antibodies were employed to immunofluorescently label formaldehyde-fixed granule cell cultures.

The use of immunofluorescence allows determination of whether the phosphorylation signal detected by immunoblotting is due to phosphorylation of a sub-population of neurones (or synaptic boutons thereof) or whether the signal is homogeneously distributed among all the synaptic boutons in the culture. Indeed, in the case of membrane depolarisation with either KCl or 4AP, the effects were widespread and the majority of synaptic boutons appeared to contain synapsin I phosphorylated on site 3. However, computer analysis of the ratio of fluorescence labelling indicated the existence of

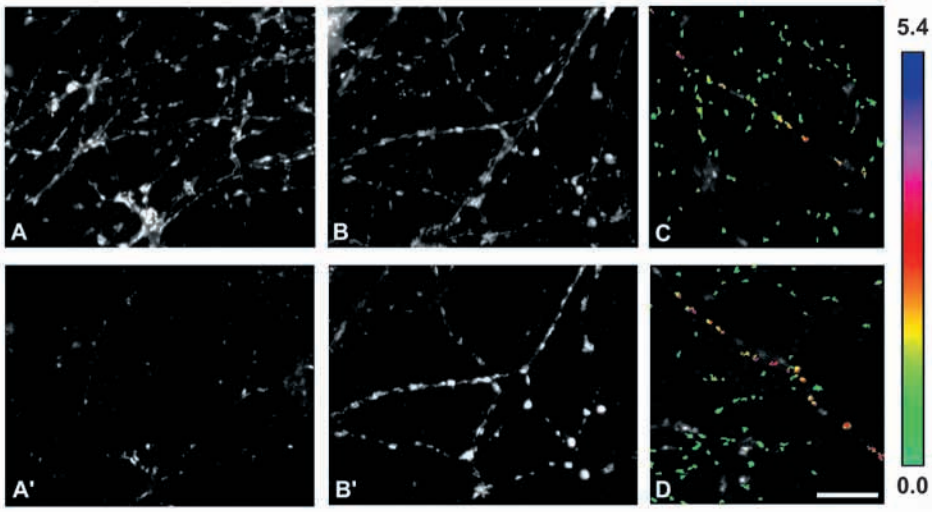

Fig. 7. Immunofluorescence-ratio imaging of forskolin-induced phosphorylation of the synapsins at site 1. Cerebellar granule cells were treated as described in the legend to Fig. 5. During the final 0.5 (B and B′), 2 (C), or 10 (D) minutes the cells were stimulated with 10 μM forskolin. (A and A′) Control samples. After formaldehyde fixation, double immunofluorescence was employed to decorate total synapsins (A and B) and phosphorylation-site 1 (A′ and B′). Some degree of site 1 phosphorylation was evident in control samples (A′). The staining increased considerably after forskolin treatment, although not all neurites appeared to be labelled (B′). (C and D) Pseudo-colour representations of the multiple of the basal phosphorylation values in selected fields of view. In each field, one neurite is present in which synapses exhibit 2- to 3-fold higher levels of site 1-phosphorylated synapsin above control. White-coloured spots were excluded from the analysis. Bars: 12.5 μm (A,A′,B,B′); 25 μm (C and D).

variability in the phosphorylation stoichiometries of individual terminals, suggesting functional heterogeneity in the phosphorylation response to Ca^{2+} influx. This was particularly true in the case of cultures treated with 4AP, where the levels of synapsin I phosphorylation appeared to be spread over a wide range. The fact that chelation of external Ca^{2+} or the application of calmodulin or CaMPKII inhibitors was sufficient to abrogate phosphorylation of synapsin I corroborates the accepted view that Ca^{2+} influx triggers the activation of calmodulin which in turn stimulates CaMPKII-mediated phosphorylation of site 3 and provides a further indication of the labelling specificity obtained with the RU19 antibody.

When tested by immunoblotting with the antibody G257, recognising phosphorylated site 1 (corresponding to Ser 9 in synapsin I and Ser 10 in synapsin II), cerebellar granule cells exhibited some degree of labelling in the absence of any stimulation, suggesting that this site is constitutively phosphorylated to some extent in this experimental system. In order to enhance phosphorylation of this site, cell cultures were treated with either dibutyryl cAMP or forskolin prior to lysis. Both agents were able to cause an increase in site 1 phosphorylation, indicating that in intact cells this site is indeed phosphorylated in response to increases in the intracellular concentration of cAMP. Although synapsin site 1 can be phosphorylated by CaMPKI, no significant increase in its phosphorylation was observed following depolarisation by either KCl or 4AP, at variance with site 3 phosphorylation by CaMPKII. As both calmodulin-dependent kinases were reported to be present in nerve terminals and exhibit similar K_m values for synapsin I (Huttner and Greengard, 1979; Huttner et al., 1981; Benfenati et al., 1992; Picciotto et al., 1995), the differential sensitivity of synapsin sites 1 and 3 to Ca^{2+} influx might be ascribed to a different compartmentalisation of substrates, kinases and kinases activators within the terminal. In this respect, it has been reported that dephosphorylated synapsin I interacts with a synaptic vesicle-associated form of CaMPKII and therefore its phosphorylation on sites 2 and 3 can occur very efficiently upon Ca^{2+} entry (Benfenati et al., 1992).

Immunofluorescence analysis revealed that the increase in site 1 phosphorylation detected by immunoblotting could be ascribed to an effect of the stimulatory agents on a sub-population of the synaptic boutons present in the preparation. The responsive boutons were aligned along individual axon branches, suggesting that they belonged to the same neurone. We do not know the reason for the selective effect of cAMP-increasing agents. Although we cannot exclude the presence of a sub-population of histologically distinct neurones, neurones in our cultures have a rather homogeneous aspect, and the vast majority of them seem to belong to the type of cerebellar granule cells (Gallo et al., 1987). Thus, it is possible that the distinct phosphorylation pattern is due to heterogeneity of nerve terminal compartments belonging to different neurones for the cAMP transduction pathway.

One advantage of the present imaging method is that it allows discrimination of whether the partial response obtained with a given pharmacological agent is due to the activation of a subset of neurones. Previously, the use of antibodies specific for the auto-phosphorylated form of CaMPKII in immunocytochemistry has been described (Kindler and Kennedy, 1996; Ouyang et al., 1997). Those antibodies are quite useful for the immunocytochemical analysis of kinase activation in neurones. However, although CaMPKII activation obviously reflects increases in intracellular Ca^{2+}, CaMPKII phosphospecific antibodies are not suitable for the analysis of $[Ca^{2+}]$ homeostasis in specific intracellular compartments. In fact, CaMPKII is present in virtually all neuronal compartments, albeit it is maximally concentrated in post-synaptic densities. In addition, the problem of the analysis of the activation of single synaptic boutons has not been addressed previously. Thus, the methodology that we have developed establishes a step forward in the study of signal transduction in neurones, and may have potential applications in various fields of neuropharmacology and neurophysiology. The possibility of visualising the activation of signal transduction pathways on a synapse-by-synapse basis may allow the detection of responses in a minor population of neurones within a complex network. In addition, it should be possible to answer the question as to whether synaptic boutons belonging to the same neurone behave in a co-ordinated manner or whether they behave independently from each other, their activity being modulated by local changes in the extracellular environment. Computer analysis of the intensity of the response in terms of synapsin I phosphorylation may also allow the detection of heterogeneous levels of synapsin I stoichiometry of phosphorylation. In addition to its usefulness in the study of neuronal cultures, the method might also have interesting applications in the intact brain, allowing the detection of the activation of synaptic terminals within a certain pathway, and its modulation upon various pharmacological treatments.

We thank Dr Raffaella Villa for contributing the D.I.C. image. This work was supported by grants from Telethon (#1000 to F.V. and #1131 to F.B.), the European Community IV Biotechnology RTD project (Bio4 CT98 0568 to F.B. and F.V.), the Harvard-Armenise Foundation, MURST (Projects 9805634227 to F.V. and 9805278229 to F.B.), and U.S.P.H.S. (Grant MH-39327 to P.G.). D.D. was the recipient of a Telethon post-doctoral fellowship (#233bs).

REFERENCES

Bähler, M. and Greengard, P. (1987). Synapsin I bundles F-actin in a phosphorylation-dependent manner. *Nature* **326**, 704-707.

Benfenati, F., Bähler, M., Jahn, R. and Greengard, P. (1989). Interaction of synapsin I with small synaptic vesicles: distinct sites in synapsin I bind to vesicle phospholipids and vesicle proteins. *J. Cell Biol.* **108**, 1863-1872.

Benfenati, F., Neyroz, P., Bähler, M., Masotti, L. and Greengard, P. (1990). Time-resolved fluorescence study of the neuron-specific phosphoprotein synapsin I. Evidence for phosphorylation-induced conformational changes. *J. Biol. Chem.* **265**, 12584-12595.

Benfenati, F., Valtorta, F., Rubenstein, J. L., Gorelick, F. S., Greengard, P. and Czernik, A. J. (1992). Synaptic vesicle-associated Ca^{2+}/calmodulin-dependent protein kinase II is a binding protein for synapsin I. *Nature* **359**, 417-420.

Boyd, I. A. and Martin, A. R. (1956). The end-plate potential in mammalian muscle. *J. Physiol.* **132**, 74-91.

Burgaya, F., Menegon, A., Menegoz, M., Valtorta, F. and Girault, J. A. (1995). Focal adhesion kinase in rat central nervous system. *Eur. J. Neurosci.* **7**, 1810-1821.

Ceccarelli, B. and Hurlbut, W. P. (1980). Ca^{2+}-dependent recycling of synaptic vesicles at the frog neuromuscular junction. *J. Cell Biol.* **87**, 297-303.

Czernik, A. J., Pang, D. T. and Greengard, P. (1987). Amino acid sequences surrounding the cAMP-dependent and calcium/calmodulin-dependent

phosphorylation sites in rat and bovine synapsin I. *Proc. Nat. Acad. Sci. USA* **84**, 7518-7522.

Czernik, A. J., Girault, J. A., Nairn, A. C., Chen, J., Snyder, G., Kebabian, J. and Greengard, P. (1991). Production of phosphorylation state-specific antibodies. *Meth. Enzymol.* **201**, 264-283.

De Camilli, P., Benfenati, F., Valtorta, F. and Greengard, P. (1990). The synapsins. *Annu. Rev. Cell Biol.* **6**, 433-460.

Dunkley, P. R., Heath, J. W., Harrison, S. M., Jarvie, P. E., Glenfield, P. J. and Rostas, J. A. (1988). A rapid Percoll gradient procedure for isolation of synaptosomes directly from an S1 fraction: homogeneity and morphology. *Brain Res.* **441**, 59-71.

Gallo, V., Suergiu, R., Giovannini, C. and Levi, G. (1987). Glutamate receptor subtypes in cultured cerebellar neurons: modulation of glutamate and gamma-aminobutyric acid release. *J. Neurochem.* **49**, 1801-1809.

Greengard, P., Valtorta, F., Czernik, A. J. and Benfenati, F. (1993). Synaptic vesicle phosphoproteins and regulation of synaptic function. *Science* **259**, 780-785.

Grynkiewicz, G., Poenie, M. and Tsien, R. Y. (1985). A new generation of Ca^{2+} indicators with greatly improved fluorescence properties. *J. Biol. Chem.* **260**, 3440-3450.

Hilfiker, S., Pieribone, V. A., Czernik, A. J., Kao, H. T., Augustine, G. J. and Greengard, P. (1999). Synapsins as regulators of neurotransmitter release. *Philos. Trans R Soc. Lond. B Biol. Sci.* **354**, 269-279.

Hosaka, M. and Südhof, T. C. (1998). Synapsin III, a novel synapsin with an unusual regulation by Ca^{2+}. *J. Biol. Chem.* **273**, 13371-13374.

Huttner, W. B. and Greengard, P. (1979). Multiple phosphorylation sites in protein I and their differential regulation by cyclic AMP and calcium. *Proc. Nat. Acad. Sci. USA* **76**, 5402-5406.

Huttner, W. B., DeGennaro, L. J. and Greengard, P. (1981). Differential phosphorylation of multiple sites in purified Protein I by cyclic AMP-dependent and calcium-dependent protein kinases. *J. Biol. Chem.* **256**, 1482-1488.

Itoh, H. and Hidaka, H. (1984). Direct interaction of calmodulin antagonists with Ca^{2+}/calmodulin-dependent cyclic nucleotide phosphodiesterase. *J. Biochem.* **96**, 1721-1726.

Jessell, T. M. and Kandel, E. R. (1993). Synaptic transmission: a bidirectional and self-modifiable form of cell-cell communication. *Cell* **72**, 1-30.

Jovanovic, J. N., Benfenati, F., Siow, Y. L., Sihra, T. S., Sanghera, J. S., Pelech, S. L., Greengard, P. and Czernik, A. J. (1996). Neurotrophins stimulate phosphorylation of synapsin I by MAP kinase and regulate synapsin I-actin interactions. *Proc. Nat. Acad. Sci. USA* **93**, 3679-3683.

Kao, H. T., Porton, B., Czernik, A. J., Feng, J., Yiu, G., Haring, M., Benfenati, F. and Greengard, P. (1998). A third member of the synapsin gene family. *Proc. Nat. Acad. Sci. USA* **95**, 4667-4672.

Katz, B. and Miledi, R. (1965). Release of acetylcholine from a nerve terminal by electric pulses of variable strength and duration. *Nature* **207**, 1097-1098.

Kindler, S. and Kennedy, M. B. (1996). Visualization of autophosphorylation of Ca^{2+}/calmodulin-dependent, protein kinase II in hippocampal slices. *J. Neurosci. Meth.* **68**, 61-70.

Laemmli, U. K. (1970). Cleavage of structural proteins during the assembly of the head of bacteriophage T4. *Nature* **227**, 680-685.

Llinas, R., Steinberg, I. Z. and Walton, K. (1981). Relationship between presynaptic calcium current and postsynaptic potential in squid giant synapse. *Biophys. J.* **33**, 323-351.

Matsubara, M., Kusubata, M., Ishiguro, K., Uchida, T., Titani, K. and Taniguchi, H. (1996). Site-specific phosphorylation of synapsin I by mitogen-activated protein kinase and Cdk5 and its effects on physiological functions. *J. Biol. Chem.* **271**, 21108-21113.

Menegon, A., Leoni, C., Benfenati, F. and Valtorta, F. (1997). Tat protein from HIV-1 activates MAP kinase in granular neurons and glial cells from rat cerebellum. *Biochem. Biophys. Res. Commun.* **238**, 800-805.

Nestler, E. J. and Greengard, P. (1984). *Protein Phosphorylation in the Nervous System*. New York: John Wiley and Sons.

Ouyang, Y., Kantor, D., Harris, K. M., Schuman, E. M. and Kennedy, M. B. (1997). Visualization of the distribution of autophosphorylated calcium/calmodulin-dependent protein kinase II after tetanic stimulatio in the CA1 area of the hippocampus. *J. Neurosci.* **17**, 5416-5427.

Petrucci, T. C. and Morrow, J. S. (1987). Synapsin I: an actin-bundling protein under phosphorylation control. *J. Cell Biol.* **105**, 1355-1363.

Picciotto, M. R., Zoli, M., Bertuzzi, G. and Nairn, A. C. (1995). Immunochemical localization of calcium/calmodulin-dependent protein kinase I. *Synapse* **20**, 75-84.

Schiebler, W., Jahn, R., Doucet, J. P., Rothlein, J. and Greengard, P. (1986). Characterization of synapsin I binding to small synaptic vesicles. *J. Biol. Chem.* **261**, 8383-8390.

Schweitzer, E. S., Sanderson, M. J. and Wasterlain, C. G. (1995). Inhibition of regulated catecholamine secretion from PC12 cells by the Ca^{2+}/calmodulin kinase II inhibitor kN-62. *J. Cell Sci.* **108**, 2619-2628.

Smith, S. J. and Augustine, G. J. (1988). Calcium ions, active zones and synaptic transmitter release. *Trends Neurosci.* **11**, 458-464.

Südhof, T. C., Czernik, A. J., Kao, H. T., Takei, K., Johnston, P. A., Horiuchi, A., Kanazir, S. D., Wagner, M. A., Perin, M. S., De Camilli, P. et al. (1989). Synapsins: mosaics of shared and individual domains in a family of synaptic vesicle phosphoproteins. *Science* **245**, 1474-1480.

Vaccaro, P., Dente, L., Onofri, F., Zucconi, A., Martinelli, S., Valtorta, F., Greengard, P., Cesareni, G. and Benfenati, F. (1997). Anti-synapsin monoclonal antibodies: Epitope mapping on mammalian synapsins using phage display libraries. *Brain Res. Mol. Brain Res.* **52**, 1-16.

Valtorta, F., Benfenati, F. and Greengard, P. (1992a). Structure and function of the synapsins. *J. Biol. Chem.* **267**, 7195-7198.

Valtorta, F., Greengard, P., Fesce, R., Chieregatti, E. and Benfenati, F. (1992b). Effects of the neuronal phosphoprotein synapsin I on actin polymerization. *J. Biol. Chem.* **267**, 11281-11288.

Valtorta, F. and Benfenati, F. (1995). Membrane trafficking in nerve terminals. *Advan. Pharmacol.* **32**, 505-557.

Valtorta, F., Benfenati, F. and Leoni, C. (1998). The synapsins and neurotransmission. In *Cellular and Molecular Mechanisms of Toxin Action. Secretory Systems* (ed. P. Lazarovici, A. Grasso and M. Linial), pp. 387-418. Amsterdam: Harwood Academic Publishers.

Weiner, N. (1979). Multiple factors regulating the release of norepinephrine consequent to nerve stimulation. *Fed. Proc.* **38**, 2193-2202.

Zucker, R. S. (1989). Short-term synaptic plasticity. *Annu. Rev. Neurosci.* **12**, 13-31.